Focal intensity landscapes of tightly focused spatially varying bright ellipse fields

OPEN ACCESS
IOP Publishing
Journal of Optics
J. Opt. **24** (2022) 044013 (7pp)
https://doi.org/10.1088/2040-8986/ac56b7

Focal intensity landscapes of tightly focused spatially varying bright ellipse fields

Sushanta Kumar Pal[1,*], **Rakesh Kumar Singh**[2,*] and **P Senthilkumaran**[3]

[1] School of Electrical Engineering, Fleischman Faculty of Engineering, Tel Aviv University, Tel Aviv 69978, Israel
[2] Laboratory of Information Photonics and Optical Metrology, Department of Physics, Indian Institute of Technology (Banaras Hindu University), Varanasi 221005, Uttar Pradesh, India
[3] Optics and Photonics Centre, Indian Institute of Technology Delhi, Hauz Khas, New Delhi 110016, India

E-mail: sushanta1985@gmail.com and krakeshsingh.phy@iitbhu.ac.in

Received 27 December 2021, revised 8 February 2022
Accepted for publication 18 February 2022
Published 11 March 2022

Abstract

Vector vortex beams play an important role in tailoring tightly focused fields by creating an additional longitudinal component at the focal plane. Until now, mainly focusing properties of fundamental, higher order vector fields and negative indexed ellipse fields have been investigated. In this paper we numerically analyze tight focusing behaviour of ellipse fields embedding C-point singularities of index $I_C = \pm\frac{1}{2}$, $I_C = \pm 1$, $I_C = \pm\frac{3}{2}$ and $I_C = \pm 2$. We show that both the sign and absolute value of C-point index (I_C) of the ellipse fields play an important role in tailoring the focal intensity landscapes. For negative index C-points the intensity distribution of the longitudinal components show symmetries that correspond to the number of separatrices present in the polarization distribution. At the focal plane, both transverse and longitudinal components of the ellipse fields are found to be embedded with phase singularities. These ellipse fields can be useful in advanced microscopy for shaping the focus of light fields for various applications.

Keywords: C-points, polarization singularity, tight focusing, structured light, optical vortices, optical singularity

(Some figures may appear in colour only in the online journal)

1. Introduction

Shaping the focal intensity landscapes of a light field has been widely considered for fundamental research and for a wide variety of applications [1]. Apart from the amplitude and phase of an optical field, the polarization parameter plays a crucial role for shaping light fields in paraxial as well as non-paraxial regime. This in turn demands the investigation of a tight focusing behaviour of structured ellipse field singularities. Structured ellipse field singularities have a myriad of advanced applications in areas such as optical trapping and manipulation [2], optical lattices [3–5], sub-Doppler laser cooling [6], material machining [7–9], high resolution microscopy [10–13], and structured illumination microscopy [14]. Understanding of tight focusing properties of structured ellipse fields, embedded with polarization singularities, will be useful for the advancement of these applications.

Tightly focused vector beams are known to produce a significant longitudinal polarization component in addition to

* Authors to whom any correspondence should be addressed.

transverse electric field components [15–18] at the focal plane. This additional longitudinal component helps in the generation of 3D-polarization structures including 3D-polarization singularities [19, 20], shaping 3D-intensity structures [21–24] and topological structures [25–28]. For example, Poincaré beams embedded with polarization singularities can be tightly focused to realize optical Mobius stripes [26, 27]. Upon tight focusing a radially polarized light creates significant longitudinal component, whereas an azimuthally polarized light stays purely transverse in nature. As a result, radially and azimuthally polarized beams are widely used [16].

Spatially varying polarization distributions can be broadly classified into two types, namely: (a) vector fields and (b) ellipse fields. Vector fields are made up of only linear states of polarization with spatially varying orientations. Singularities of the vector fields are known as V-points and they are characterized by the Poincaré-Hopf index (η). The V-point index (η) can be expressed as $\eta = \frac{1}{2\pi}\oint \vec{\nabla}\gamma_0 \cdot \vec{dl}$, where γ_0 is the orientation of the linear polarization around the singular point. V-points are points of undefined polarization, where the orientation of linear polarization is undefined [24, 29–31]. These are intensity nulls in the intensity distribution. In contrast, the predominant states of polarization in an ellipse field are ellipses. The singularities of an ellipse field are known as C-points and these singularities are defined by an index called as C-point index (I_C) [31–35]. The C-point index ((I_C) is given by, $I_C = \frac{1}{2\pi}\oint \vec{\nabla}\gamma_0 \cdot \vec{dl}$, where γ_0 is the azimuth of the polarization ellipse. C-points are the points of undefined azimuths, at which the state of polarization (SOP) is circular. Ellipse fields whose spatially variant polarization states span the whole Poincaré sphere are called as Full Poincaré beams [36–39]. Polarization distribution of such beams occupies different spatial regions on the surface of the Poincaré sphere. If the extent of the occupancy of states on the Poincaré sphere is partial, they are generally termed as Poincaré beams. In general, these beams can be represented as a superposition of orthogonally polarized modes such as Laguerre-Gauss or Bessel beams with the same frequency. As a result, the local polarization of Poincaré beams, which may be linear, elliptical, and circular, varies both azimuthally and radially. Recently Full Poincaré beams are characterized by using hybrid order Poincaré sphere [37]. Tight focusing properties of these fields have not been studied to the best of our knowledge and investigation of these fields is important.

In this article, we investigate the tight focusing properties of generic and higher order ellipse field singularities such as stars, lemons, and radial C-points and, thereby, realize structured three-dimensional focal field distributions. Monstar has anisotropic ϕ_{12} Stokes field phase distribution and hence are not studied here. The relative phase difference between the orthogonal field components has been referred to as the Stokes phase in literature [40]. Based on the choice of basis system there are three types of Stokes phase distributions, namely ϕ_{12}, ϕ_{23} and ϕ_{31}, respectively [40]. For an inhomogenously polarized light beam the Stokes phase is a distribution. The singularities present in the Stokes phase distribution are called Stokes singularities or Stokes vortices. We show that both the sign and absolute value of the C-point index (I_C) of the ellipse field singularities play an important role in tailoring the focal intensity landscapes.

2. Tight focusing of bright C-points

Ellipse fields embedded with C-point singularities can be generated by the superposition of beams in two orthogonal circular basis [41, 42]—one or both carrying orbital angular momentum (OAM) and are given by,

$$\begin{aligned}\vec{E}(r,\theta) &= \Psi_L \hat{e}_L + \Psi_R \hat{e}_R \\ &= B_1 r^{|m|} e^{im\theta}\hat{e}_L + B_2 r^{|n|} e^{i(n\theta+\theta_0)}\hat{e}_R,\end{aligned} \tag{1}$$

where $\hat{e}_L$ and $\hat{e}_R$ are the left and right circular unit basis vectors, respectively. In equation (1) m, n are the topological charges of the phase vortex beams with amplitude scaling factors B_1 and B_2 respectively. The intrinsic OAM carried by orthogonal circular basis states are $m\hbar$ and $n\hbar$ per photon. In equation (1), θ is the azimuthal angle, and θ_0 is the initial phase shift given to one of the beams. Here, left (right) handed circularly polarized light carries spin angular momentum equal to $+\hbar$ ($-\hbar$) per photon. In the cartesian basis (xy-basis) equation (1) can be expressed as

$$\begin{aligned}\vec{E}(x,y) &= \frac{1}{\sqrt{2}}[C(x,y)\hat{e}_x - iD(x,y)\hat{e}_y] \\ C(x,y) &= \left[B_1 r^{|m|} e^{im\theta} + B_2 r^{|n|} e^{i(n\theta+\theta_0)}\right] \\ D(x,y) &= \left[B_1 r^{|m|} e^{im\theta} - B_2 r^{|n|} e^{i(n\theta+\theta_0)}\right].\end{aligned} \tag{2}$$

Tight focusing of polarization modulated optical fields can reveal additional properties due to the presence of significant longitudinal polarization components (E_z) of the electric field within the focal volume. Recently, vector fields embedded with higher order V-points such as flowers and webs have been used to shape the focal spot intensity distribution [43]. We apply the numerical method to study the tight focusing properties of ellipse fields embedded with C-point singularities (equation (2)), which is yet to be investigated. The amplitude of a Gaussian beam at the entrance pupil of the lens is given by

$$E_1(\rho) = E_0 e^{-\gamma^2 \rho^2}, \tag{3}$$

where E_0 is the amplitude corresponding to maximum intensity of the beam, ρ is the radial distance of a point from the centre normalized by the radius (a) of the lens. $\gamma = a/w$ is the truncation parameter which denotes the fraction of the beam inside the physical aperture of the lens, where w is the beam waist. Equation (3) can be written in terms of the conic angle ϕ as

$$E_2(\phi) = E_0 e^{(-\gamma^2 \sin^2\phi/\sin^2\alpha)}, \tag{4}$$

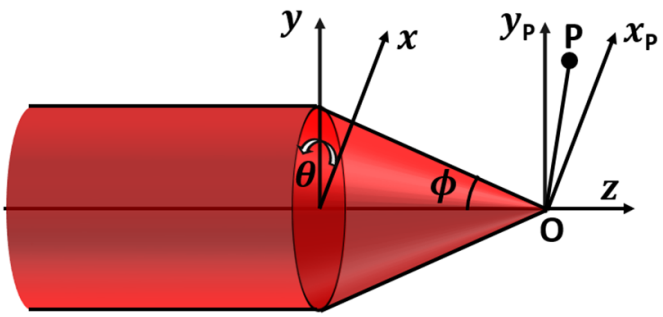

Figure 1. Geometric configuration for tight focusing. Optical coordinates at the observation plane and entrance pupil plane of the lens is given by (x_p,y_p) and (x,y) respectively. ϕ is the focusing angle and θ is the azimuthal angle.

where $\rho = \sin\phi/\sin\alpha$, ϕ is the focusing angle and α is the maximum angle of convergence ($\phi_{max} = \alpha$). The numerical aperture (NA) of an optical system is given by $NA = n\sin\alpha = n\sin\phi_{max}$, where n is the refractive index of the focal region. For a focusing configuration shown in figure 1, the electric field components in the focal region of an aberration free aplanatic lens system is given by [44–46]

$$E(u,\upsilon) = (-iA/\lambda)\int_0^{\alpha}\int_0^{2\pi} E_2(\phi)P(\phi,\theta)A_2(\phi) \times e^{\left(-i\frac{\upsilon}{\sin\alpha}\sin\phi\cos(\theta-\theta_P)\right)} \times e^{\left(-i\frac{u}{\sin^2\alpha}\cos\phi\right)}\sin\theta d\phi d\theta, \quad (5)$$

where A is linked to the optical system parameters and λ is the wavelength of light in the medium with refractive index (n) in the focal region. $P(\phi,\theta)$ denotes polarization distribution at the exit pupil and $A_2(\phi)$ is the apodization factor. For an aplanatic lens system $A_2(\phi)$ is $\cos^{\frac{1}{2}}\phi$. We assume that the normals to the ideal and the actual wavefront point in the same direction. The polarization distribution of the input field can be expressed as

$$P(\phi,\theta) = \begin{pmatrix} a_1\ C_1 + b_1\ C_2 \\ a_1\ C_2 + b_1\ C_3 \\ -a_1\ \sin\phi\cos\theta - b_1\ \sin\phi\sin\theta \end{pmatrix}, \quad (6)$$

where $C_1 = \cos\phi\cos^2\theta + \sin^2\theta$, $C_2 = \cos\phi\sin\theta\cos\theta - \sin\theta\cos\theta$, $C_3 = \cos\phi\sin^2\theta + \cos^2\theta$, a_1 and b_1 are the strengths of the x and y components of the input field respectively. Optical coordinates at the observation plane are defined as

$$u = kz\sin^2\alpha$$
$$\upsilon = k\sin\alpha\sqrt{x_P^2 + y_P^2}, \quad (7)$$

where $k = 2\pi/\lambda$. We consider an optical system with NA 0.95 to demonstrate the focal plane intensity distribution of various ellipse field singularities. We used the Matlab code to numerically evaluate the Debye-Wolf integral (equation (5)) for a given input beam in a cylindrical co-ordinate system. In order to implement this numerical integration, we discretized

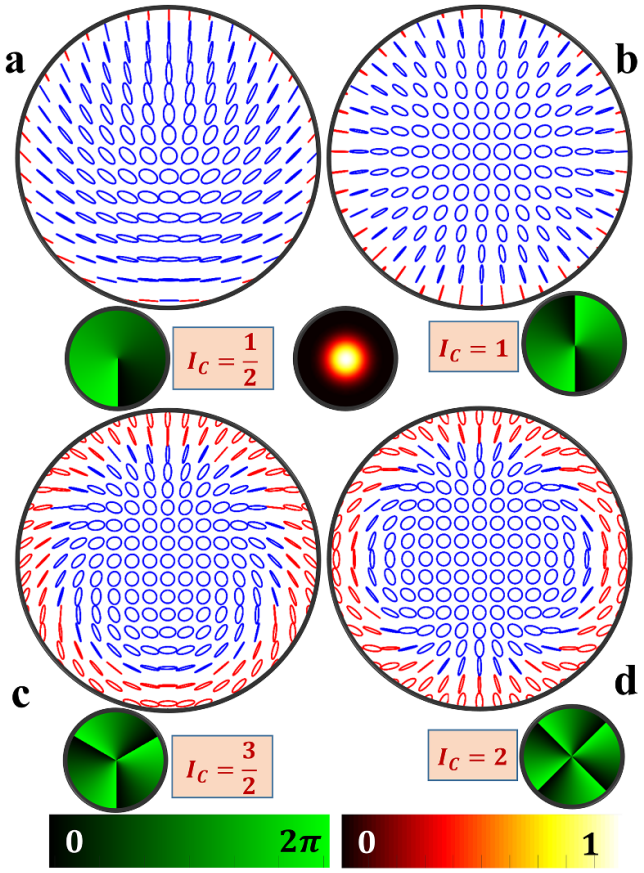

Figure 2. Simulated polarization distributions of various ellipse field singularities with different C-point index. (a) $I_C = \frac{1}{2}$ C-point; (b) $I_C = 1$ C-point; (c) $I_C = \frac{3}{2}$ C-point; and (d) $I_C = 2$ C-point respectively. The S_{12} Stokes field phase distribution and intensity distribution of all these four ellipse fields are shown as insets.

the exit pupil function into the azimuthal and radial segments. Detailed numerical calculations to evaluate the integrals can be found in [47] and this reference has been included in the revised manuscript. The polarization distributions, total intensity distributions and Stokes phase distributions are calculated using equation (1). The azimuth and ellipticity distributions are obtained using Stokes parameters, which are further used to plot the SOP at each point in the beam. At the focal plane the x, y and z components of the input ellipse field are calculated using equation (5). The polarization distribution of four different types of ellipse filed singularities are shown in figure 2. All these four ellipse fields have the same intensity distribution and this is shown as the inset in figure 2. Polarization distributions of a lemon ($I_C = +1/2$) and radial C-point ($I_C = +1$) are depicted in figures 2(a) and (b) respectively. Figures 2(c) and (d) show the polarization distribution of the $I_C = 3/2$ and $I_C = 2$ C-points, respectively. The corresponding S_{12} Stokes field phase distributions are shown as insets.

Figure 3 depicts the focal plane intensity distributions corresponding to transverse and longitudinal components of different ellipse field singularities. In figure 3, all the intensity structures are normalized with respect to the maximum value of the total intensity. The intensities corresponding to

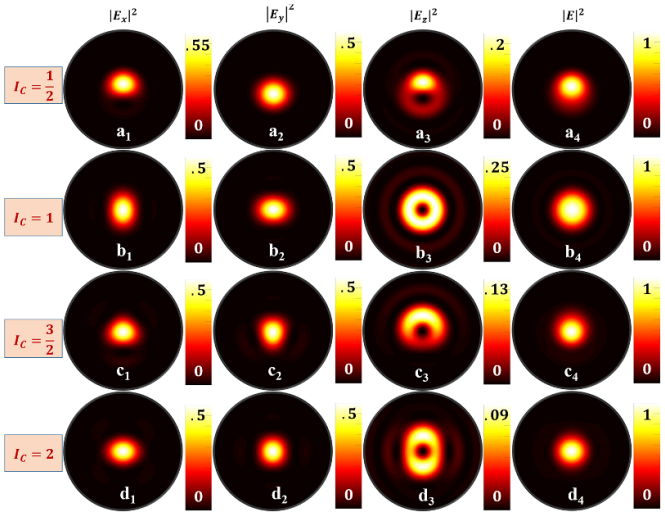

Figure 3. Tight focusing (NA = 0.95) of ellipse field singularities as shown in figure 2. For each ellipse field distributions: $(a_1 - a_4)$ $I_C = \frac{1}{2}$; $(b_1 - b_4)$ $I_C = 1$; $(c_1 - c_4)$ $I_C = \frac{3}{2}$; and $(d_1 - d_4)$ $I_C = 2$ the focal plane intensity distributions corresponding to x, y and z-components are shown in column I ($|E_x|^2$), column II ($|E_y|^2$) and column III ($|E_z|^2$) respectively. Total intensity ($|E|^2$) distributions are shown in column IV.

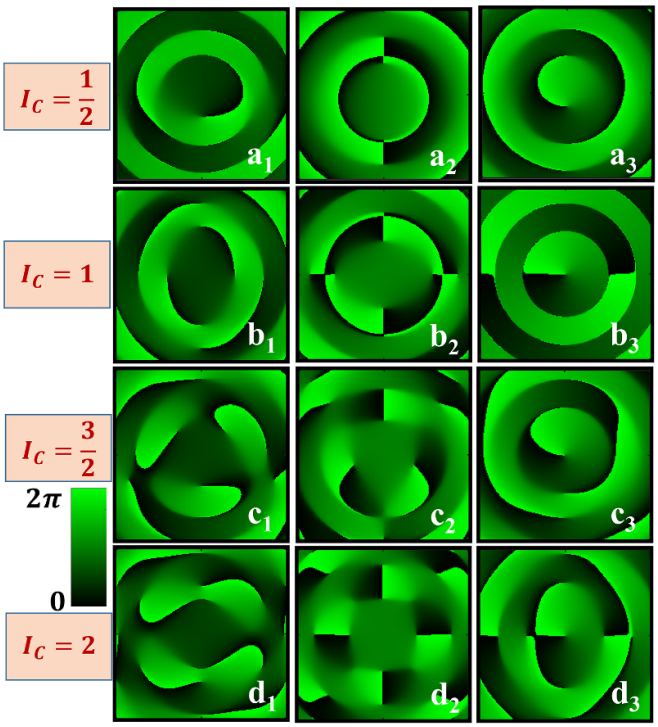

Figure 4. Focal plane phase distributions corresponding to E_x, E_y and E_z-component of each ellipse field singularities are shown in figure 4. For each ellipse field distributions: $(a_1 - a_3)$ $I_C = \frac{1}{2}$; $(b_1 - b_3)$ $I_C = 1$; $(c_1 - c_3)$ $I_C = \frac{3}{2}$; and $(d_1 - d_3)$ $I_C = 2$ the focal plane phase distributions corresponding to E_x, E_y and E_z-components are shown in column I, column II and column III respectively.

x and y components of the fields, at the focal plane, are shown in column I and column II respectively. The intensities corresponding to the longitudinal components (E_z) of the fields are shown in column III. For each polarization distribution, the total intensity distributions are shown in column IV. Row I and row II of figure 3 correspond to lemon $\left(I_C = \frac{1}{2}\right)$ (figure 2(a)) and radial ($I_C = 1$) (figure 2(b)) C-points, respectively. Interestingly, the intensity distribution corresponding to the longitudinal component of the $I_C = 1$ ellipse field singularity resembles the total intensity that can be obtained using the Laguerre–Gaussian mode. Intensity distributions corresponding to C-points with $I_C = \frac{3}{2}$ (figure 2(c)) and $I_C = 2$ (figure 2(d)) are shown in row III and row IV, respectively. By using figures 2 and 3 one can observe that the focal plane intensity distribution is dependent on the absolute value of the C-point index, which is very interesting. Figure 4 depicts the focal plane phase distributions corresponding to the transverse and longitudinal components of different ellipse field singularities. At the focal plane, all the field components are found to be embedded with number of phase singularities. The physical origin of these phase vortices may be due to the mixing of polarization components of the electric field in the tight focusing situation. This interplay between the polarization components may lead to the formation of phase vortices in the component fields. Next, the effect of sign of C-point index in the focal plane intensity distribution is studied.

The polarization, intensity and S_{12} Stokes field phase distributions of index inversed ellipse field singularities of figure 2 are shown in figure 5. The focal plane intensity distributions corresponding to the transverse and longitudinal components of these ellipse field singularities are shown in figure 6, where all the intensity distributions are normalized with respect to the maximum value of the total intensity. The intensities corresponding to transverse components (x and y components) of the fields, at the focal plane, are shown in column I and column II respectively. The intensities corresponding to the longitudinal components (E_z component) of all the fields are presented in column III. For each polarization distribution the total intensity distributions are shown in column IV. Row I and row II of figure 6 correspond to star ($I_C = \frac{-1}{2}$) and type IV C-points ($I_C = -1$), respectively. In figure 6, the focal plane intensity distributions corresponding to transverse and longitudinal components of ellipse field singularities with $I_C = \frac{-3}{2}$ and $I_C = -2$ are shown in row III and row IV, respectively. The focal plane phase distributions corresponding to the transverse and longitudinal components of index inversed ellipse field singularities are shown in figure 7. At the focal plane both transverse and longitudinal components of the index inversed fields are embedded with phase singularities.

A comparison between focal plane intensity distributions shown in figures 3 and 6, reveals there is a strong dependence on the sign of the C-point index of the beam that is focused. Interestingly for negative index C-points, the intensity distribution of the longitudinal components show symmetries that correspond to the number of separatrices present in the polarization distribution. In the case of some of the positive index C-points, the number of separatrices are such that they terminate at the centre, which may be responsible for the appearance of radial cut(s) in the longintudinal component. Since the C-point

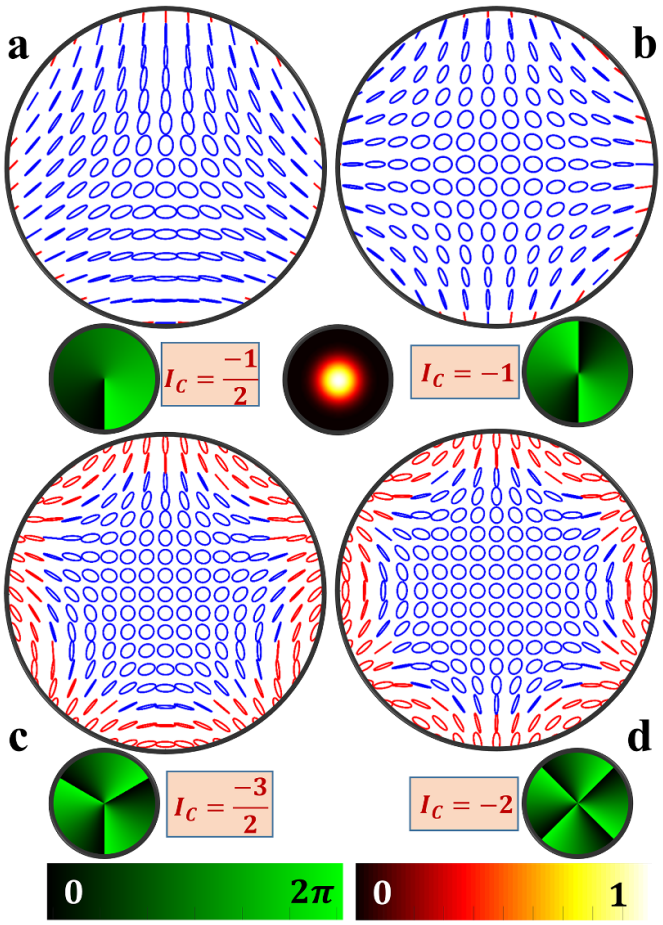

Figure 5. Simulated index inversed polarization distributions of various ellipse fields: (a) $I_C = \frac{-1}{2}$ C-point; (b) $I_C = -1$ C-point; (c) $I_C = \frac{-3}{2}$ C-point; and (d) $I_C = -2$ C-point respectively. The S_{12} Stokes field phase distribution and intensity distribution of all these four ellipse fields are shown as insets.

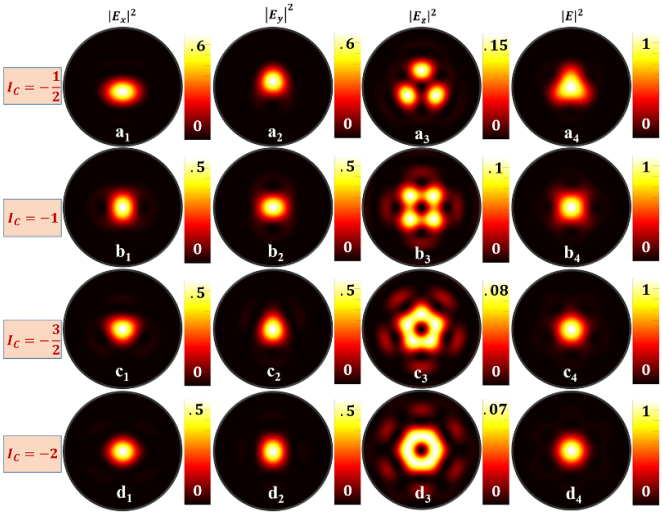

Figure 6. Tight focusing (NA = 0.95) of index inversed ellipse field singularities as shown in figure 5. For each ellipse field distributions: $(a_1 - a_4)$ $I_C = \frac{-1}{2}$; $(b_1 - b_4)$ $I_C = -1$; $(c_1 - c_4)$ $I_C = \frac{-3}{2}$; and $(d_1 - d_4)$ $I_C = -2$, the focal plane intensity distributions corresponding to x, y and z-components are shown in column I ($|E_x|^2$), column II ($|E_y|^2$) and column III ($|E_z|^2$) respectively. Total intensity ($|E|^2$) distributions are shown in column IV.

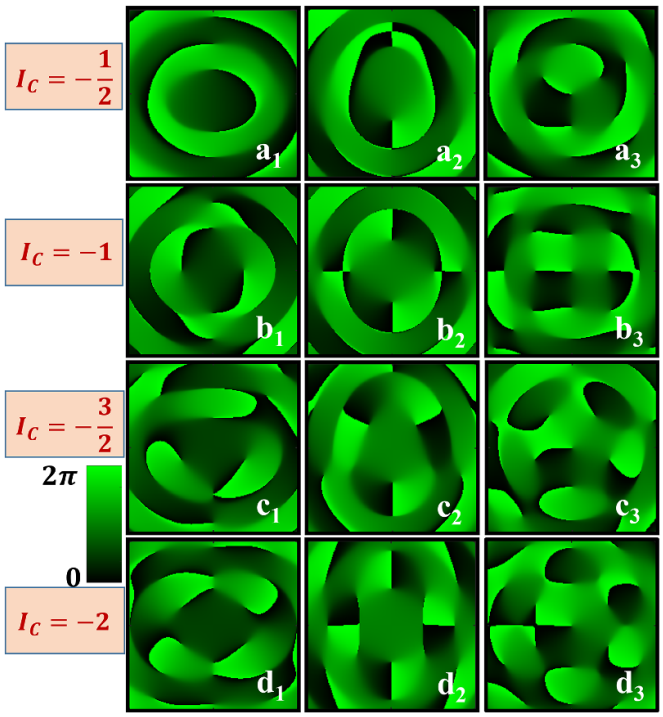

Figure 7. Focal plane phase distributions corresponding to E_x, E_y and E_z-component of index inversed ellipse field singularities are shown in figure 7. For each ellipse field distributions: $(a_1 - a_3)$ $I_C = \frac{-1}{2}$; $(b_1 - b_3)$ $I_C = -1$; $(c_1 - c_3)$ $I_C = \frac{-3}{2}$; and $(d_1 - d_3)$ $I_C = -2$ the focal plane phase distributions corresponding to E_x, E_y and E_z-components are shown in column I, column II and column III respectively.

with $I_C = 1$ does not have any separatrix, the Z-component focal plane intensity distribution for this case is circularly symmetric.

3. Conclusions

In conclusion, we numerically demonstrated the focal plane intensity landscapes of various ellipse field singularities for a high NA (NA = 0.95) system. We found that both the sign and absolute value of the C-point index (I_C) of the ellipse field singularities play a crucial role in tailoring the focal intensity distributions. It is shown that in case of negative index C-points, the intensity distribution of the longitudinal components show a similarity that corresponds to the number of separatrices present in the polarization distribution. The focal shaping of these singularities will be useful for multiple applications in optical micromanipulation, material machining or high-resolution microscopy.

Data availability statement

The data generated and/or analysed during the current study are not publicly available for legal/ethical reasons but are available from the corresponding author on reasonable request.

Acknowledgment

R K Singh acknowledge the Council of Scientific and Industrial Research (CSIR), India, for research Grant $(80(0092)/20/EMR - II)$.

ORCID iDs

Sushanta Kumar Pal https://orcid.org/0000-0001-5077-2373
Rakesh Kumar Singh https://orcid.org/0000-0002-3117-2695
P Senthilkumaran https://orcid.org/0000-0002-1015-0710

References

[1] Rubinsztein D H *et al* 2016 *J. Opt.* **19** 013001
[2] Cipparrone G, Ricardez V I, Pagliusi P and Provenzano C 2010 *Opt. Express* **18** 6008–13
[3] Chen Y h, Wu W, Liu G c, Tao H s and Liu W m 2012 *Front. Phys.* **7** 2
[4] Fölling S, Trotzky S, Cheinet P, Feld M, Saers R, Widera A, Müller T and Bloch I 2007 *Nature* **448** 1029–32
[5] Pal S K and Senthilkumaran P 2016 *Opt. Express* **24** 28008–13
[6] Dalibard J and Cohen T C 1989 *J. Opt. Soc. Am.* B **6** 2023–45
[7] Nivas J J *et al* 2017 *Sci. Rep.* **7** 42142
[8] Meier M, Romano V and Feurer T 2007 *Appl. Phys.* A **86** 329–34
[9] Rose P, Diebel F, Boguslawski M and Denz C 2013 *Appl. Phys. Lett.* **102** 101101
[10] Novotny L, Beversluis M R, Youngworth K S and Brown T G 2001 *Phys. Rev. Lett.* **86** 5251–4
[11] Hell S W and Wichmann J 1994 *Opt. Lett.* **19** 780–2
[12] Kozawa Y, Matsunaga D and Sato S 2018 *Optica* **5** 86–92
[13] Kozawa Y, Hibi T, Sato A, Horanai H, Kurihara M, Hashimoto N, Yokoyama H, Nemoto T and Sato S 2011 *Opt. Express* **19** 15947–54
[14] Xu L, Zhang Y, Lang S, Wang H, Hu H, Wang J and Gong Y 2021 *J. Innov. Opt. Health Sci.* **14** 2050027
[15] Dorn R, Quabis S and Leuchs G 2003 *Phys. Rev. Lett.* **91** 233901
[16] Youngworth K S and Brown T G 2000 *Opt. Express* **7** 77–87
[17] Kozawa Y and Sato S 2007 *J. Opt. Soc. Am.* A **24** 1793–8
[18] Kozawa Y and Sato S 2006 *Opt. Lett.* **31** 820–2
[19] Zhang W, Liu S, Li P, Jiao X and Zhao J 2013 *Opt. Express* **21** 974–83
[20] Schoonover R W and Visser T D 2006 *Opt. Express* **14** 5733–45
[21] Zhan Q and Leger J R 2002 *Appl. Opt.* **41** 4630–7
[22] Chen W and Zhan Q 2006 *Opt. Commun.* **265** 411–17
[23] Bokor N and Davidson N 2006 *Opt. Lett.* **31** 149–51
[24] Zhan Q 2009 *Adv. Opt. Photon.* **1** 1–57
[25] Dennis M R 2011 *Opt. Lett.* **36** 3765–7
[26] Bauer T, Banzer P, Karimi E, Orlov S, Rubano A, Marrucci L, Santamato E, Boyd R W and Leuchs G 2015 *Science* **347** 964–6
[27] Bauer T, Neugebauer M, Leuchs G and Banzer P 2016 *Phys. Rev. Lett.* **117** 013601
[28] Freund I 2005 *Opt. Commun.* **249** 7–22
[29] Senthilkumaran P 2018 *Singularities in Physics and Engineering* (Bristol: IOP Publishing) pp 2053–563
[30] Otte E, Alpmann C and Denz C 2016 *J. Opt.* **18** 074012
[31] Freund I 2002 *Opt. Commun.* **201** 251–70
[32] Hajnal J V and Nye J F 1987 *Proc. R. Soc.* A **414** 433–46

[33] Hajnal J V and Nye J F 1987 *Proc. R. Soc.* A **414** 447–68
[34] Dennis M R 2002 *Opt. Commun.* **213** 201–21
[35] Berry M V 2004 *J. Opt. A: Pure Appl. Opt.* **6** 475–81
[36] Beckley A M, Brown T G and Alonso M A 2010 *Opt. Express* **18** 10777–85
[37] Ling X, Yi X, Dai Z, Wang Y and Chen L 2016 *J. Opt. Soc. Am.* B **33** 2172–6
[38] Zhu W, Shvedov V, She W and Krolikowski W 2015 *Opt. Express* **23** 34029–41
[39] Arora G, Ruchi and Senthilkumaran P 2019 *Opt. Lett.* **44** 5638–41
[40] Ruchi Senthilkumaran P and Pal S K 2020 *Int. J. Opt.* **2020** 2812803
[41] Pal S K, Ruchi and Senthilkumaran P 2017 *Appl. Opt.* **56** 6181–90
[42] Cardano F, Karimi E, Marrucci L, de Lisio C and Santamato E 2013 *Opt. Express* **21** 8815–20
[43] Otte E, Tekce K, Lamping S, Ravoo B J and Denz C 2019 *Nat. Commun.* **10** 4308
[44] Richards B and Wolf E 1959 *Proc. R. Soc.* A **253** 358–79
[45] Boruah B and Neil M 2009 *Opt. Commun.* **282** 4660–7
[46] Singh R K, Senthilkumaran P and Singh K 2009 *J. Opt. Soc. Am.* A **26** 576–88
[47] Singh R K 2010 *Investigations on Tight Focusing of Singular Beams: Effect of Primary Aberrations* (Germany: Lambert Academic Publishing)